

Structural refinement of 00Cr13Ni5Mo2 supermartensitic stainless steel during single-stage intercritical tempering

Da-kun Xu, Yong-chang Liu, Zong-qing Ma, Hui-jun Li, and Ze-sheng Yan

State Key Laboratory of Hydraulic Engineering Simulation and Safety, School of Material Science and Engineering, Tianjin University, Tianjin 300072, China
(Received: 22 September 2013; revised: 24 November 2013; accepted: 25 November 2013)

Abstract: The 00Cr13Ni5Mo2 supermartensitic stainless steel was first tempered at 570–730°C for 2 h to observe the microstructure and hardness changes. The tempering temperature was set to 600, 650, and 700°C, which is below, equal to, and above the austenite transformation start temperature, respectively, for each holding period to investigate the effects of tempering time on the structure and properties of the steel. The microstructure of the specimens was examined by optical microscopy and transmission electronic microscopy, and the phase composition was detected by X-ray diffraction. As expected, lath refinement was observed in the steel tempered at 700°C, and the refinement degree significantly depended on the tempering time. Contrary to normal steel softening by tempering, the hardness performance of the steel was significantly enhanced primarily because of the refinement of martensite laths after single-stage intercritical tempering. It is believed that the reverse transformation of martensite (α') to austenite (γ) is responsible for the refinement.

Keywords: stainless steel; tempering; retained austenite; phase transitions

1. Introduction

In view of its unique combination of weldability, strength, toughness, and corrosion resistance [1], low-carbon martensitic stainless steel, also known as supermartensitic stainless steel (SMSS), was considered as an economical alternative for duplex stainless steel [2]. Nowadays, SMSS has displayed an ever-growing application value as a pipeline source material for use in the oil and gas industry, especially in CO₂- and H₂S-containing environments. SMSS is developed on the basis of a Fe–Cr–Ni–Mo alloying system with significantly reduced carbon content ($\leq 0.02\text{wt}\%$), by varying microalloying and nitrogen addition [3]. The microstructure of SMSS commonly consists of tempered lath martensite and a certain amount of retained austenite depending on the carbon content, austenite-stabilizing elements, and heat treatment parameters [4]. To achieve the ideal microstructure, the steel is generally subjected to solution treatment at 1000–1100°C followed by air/water quenching to room temperature and single- or two-stage tempering [1, 5].

For promoting the partial reverse transformation of

martensite (α') to austenite (γ), the tempering of 13Cr SMSS is often imposed at a temperature slightly above the austenite transformation start (A_s) temperature, and the process is called intercritical tempering [6]. The reversed austenite normally forms along martensite interlath boundaries and prior austenite grain boundaries, and during subsequent cooling to room temperature, it is retained in the form of thin islands dispersed between the boundaries and reaches a certain volume fraction [6–8]. Previous studies reported that the tempering temperature and time have an important effect on the strength, toughness, and pitting corrosion resistance of 13Cr SMSS by adjusting the amount of retained austenite at room temperature and the precipitating behavior of second-phase particles [9–12].

Qin *et al.* [3] found that in SMSS, the hardness value showed a steady decrease with increasing tempering temperature because of a combined effect of secondary hardening and formation of reversed austenite during tempering. In the study of Liu *et al.* [13], the hardness of 13Cr SMSS initially reduced and then increased as the tempering temperature upgraded from 550°C to 750°C, and the researchers ascribed this variation to the fluctuation of the retained austenite.

ite content, which increased first and then decreased with the increase of the tempering temperature. Zou *et al.* [11] extensively investigated the influence of the tempering process on the mechanical properties of 00Cr13Ni4Mo SMSS by tempering the steel at various temperatures and for various periods at 600°C. The hardness steadily increased as the tempering temperature elevated from 520°C to 720°C and the martensitic structure exhibited refined characteristics up to 600°C, while martensite laths coarsened after tempering in the range of 600–720°C [11]. In a number of other investigations, a refined martensitic matrix containing a certain amount of retained austenite was obtained after two-stage tempering [2, 8, 14]. However, there are only a few studies focusing on the refinement of martensitic steel and its influence on the mechanical properties of SMSS subjected to single-stage tempering.

In this study, the microstructural evolution of 00Cr13Ni5Mo2 SMSS undergoing various tempering conditions was investigated to clarify the correlation between the refinement of martensitic steel and reverse austenite transformation in the intercritical region.

2. Experimental

The steel for this study, whose chemical composition is listed in Table 1, was provided by Tianjin Pipe Corporation. The material was machined into a block with dimensions of 100 mm × 50 mm × 20 mm for solution treatment. The austenite transformation start (A_s) temperature and finish (A_f) temperature were measured by using a high-precision differential thermal analysis (DTA) apparatus by heating a specimen of size $\phi 5$ mm × 2 mm to 1050°C at a constant rate of 60°C/min; the measured A_s (650°C) and A_f temperature (800°C) are denoted by arrows in the acquired DTA curve shown in Fig. 1. The experimental steel was solution-treated at 1050°C for 1 h, followed by water quenching to room temperature to obtain a full martensitic structure. The quenched steel block was then machined into small chips with dimensions of 20 mm × 10 mm × 10 mm, which were tempered at 570, 600, 630, 650, 700, and 730°C for 2 h. With respect to the A_s temperature of the steel, another group of quenched specimens were tempered at three selected temperatures (i.e., 600, 650, and 700°C) for various periods (i.e., at 600°C for 2, 4, 6, 8 h; at 650°C for 0.5, 1, 2, 4, 6, 8 h; and at 700°C for 5, 10, 20, 30 min).

Table 1. Chemical composition of the steel investigated wt%

C	Si	Mn	Mo	Cr	Ni	Ti	Cu	Al	N
0.015	0.200	0.700	2.200	12.700	5.800	0.140	0.100	0.070	0.012

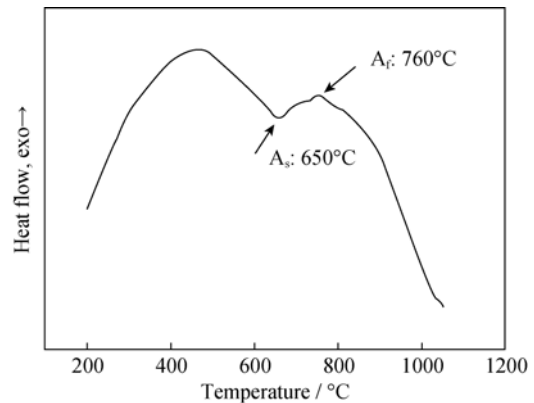


Fig. 1. DTA curve of the specimen heated to 1050°C at 60°C/min.

To characterize the microstructure of the heat-treated steel by optical microscopy (OM), the specimens were prepared by standard grinding and polishing procedures followed by etching with Kalling's reagent (CuCl₂ 1.5 g + HCl 33 mL + ethanol 33 mL + H₂O 33 mL). The morphology of the specimens was observed with a C-35A Olympus optical microscope. To further characterize martensite laths, transmission electronic microscopy (TEM; JEOL-100CX-II) was employed. For TEM observations, the specimens were first cut into 300- μ m-thick slices, then mechanically polished to about 50- μ m-thick foils, and finally electrochemical thinned by a twin-jet polisher in a 5vol% perchloric acid + 95vol% ethanol solution.

X-ray diffraction (XRD) analysis was carried out with a Bruker D8 Advance diffractometer using Cu K α radiation. The volume fraction of the retained austenite at room temperature was estimated by the following equations [15]:

$$V_\gamma + V_{\alpha'} = 1 \quad (1)$$

$$V_\gamma = \frac{1.4I_\gamma}{I_{\alpha'} + 1.4I_\gamma} \quad (2)$$

where V_γ and $V_{\alpha'}$ are the volume fractions of austenite and martensite, respectively, and I_γ and $I_{\alpha'}$ represent the integrated intensities of the (111) γ and (110) α' peaks, respectively. Vickers microhardness values were obtained by averaging the values of 10 random measurements obtained using an Everone Mh-6L hardness tester with a load of 0.49 N and a dwell time of 5 s.

3. Results and discussion

3.1. The quenched specimen

Fig. 2(a) shows the optical microstructure of the experimental steel solution-treated at 1050°C and subsequently water-quenched to room temperature. The specimen dem-

onstrated typical low-carbon martensite morphology with the original austenite grains divided into packets and blocks containing similarly oriented martensite laths, which was further characterized by TEM (see Fig. 2(b)). As shown in

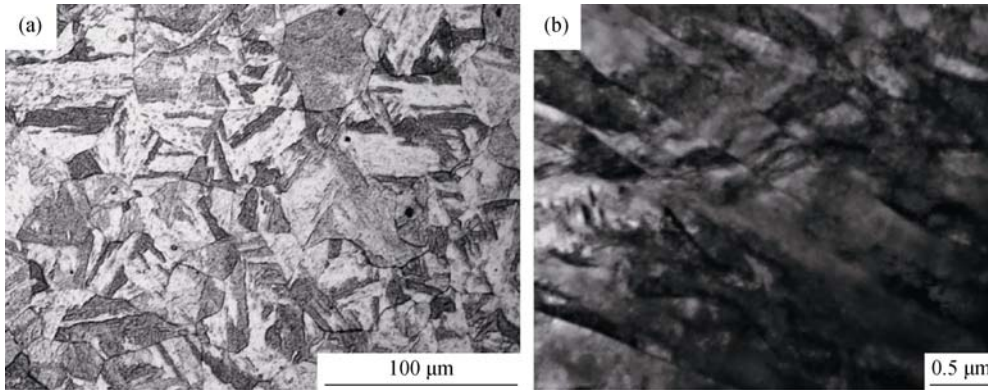


Fig. 2. Microstructures of the specimen subjected to solution treatment at 1050°C and subsequent water quenching to room temperature: (a) OM image and (b) TEM image.

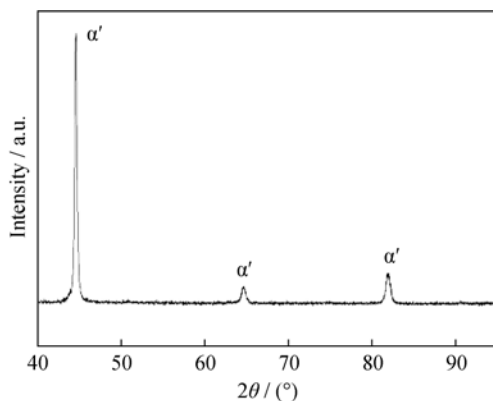


Fig. 3. XRD pattern of the specimen subjected to solution treatment at 1050°C and subsequent water quenching to room temperature.

3.2. Tempering at various temperatures

The OM images of the specimens tempered at 570–730°C are shown in Fig. 4. When the specimens were tempered in the range of 570–630°C, the packets and blocks of martensite laths had intensive contrast and the etching depth became stronger as the tempering temperature escalated. Surprisingly, starting from 650°C (see Fig. 4(d)), the morphology showed a very sharp change. For the specimens tempered at and above 650°C, although the block-like structure remained, significant refinement of the martensite lath was apparent, which was characterized in detail by TEM (see Fig. 5). The martensite lath of the specimen tempered at 650°C was notably narrowed compared with that of the quenched one, and a further reduction of the martensite lath width was observed when the specimen was tempered

the TEM image, the steel completely consists of martensite laths paralleled to each other, while no retained austenite is recognized, which is in agreement with the XRD pattern shown in Fig. 3.

at 730°C. It should be also noted that no retained austenite or precipitates were detected by TEM and XRD analysis. Fig. 6 shows the variation of the Vickers microhardness value with the temperature for the specimens tempered at different temperatures. The hardness initially decreases in the temperature range from 570 to 630°C, and this decrease is attributed to the increase of the retained austenite volume fraction [16]. Since no retained austenite was proved to be present in the specimens, the variation of hardness was unlikely to be associated with the softening of the retained austenite, but was due to the release of internal stress and elimination of dislocations in the martensitic structure [17–18]. Moreover, there was a steep increase of hardness after 650°C, which was consistent with the refinement of martensite. According to the results reported by Lee *et al.* [19], secondary hardening effect in tempering only occurred up to 450°C; therefore, the refining of martensite was considered as the reason of hardness enhancement. Refined martensite laths lead to the increase of hardness/strength by introducing more boundaries that can obstruct the movement of dislocations [20]. Blimes *et al.* [8] reported that, for 13Cr SMSS, the retained austenite generated after reverse transformation during intercritical tempering is often accompanied by lath refinement at room temperature. Considering that the refined martensite was observed only for specimens subjected to intercritical tempering, it is reasonable to infer that the reverse transformation, which occurs at temperatures above A_s temperature, led to lath refinement: the martensite lath width was reduced as a result of unstable reverse austenite re-transformation to fresh martensite during the cooling process.

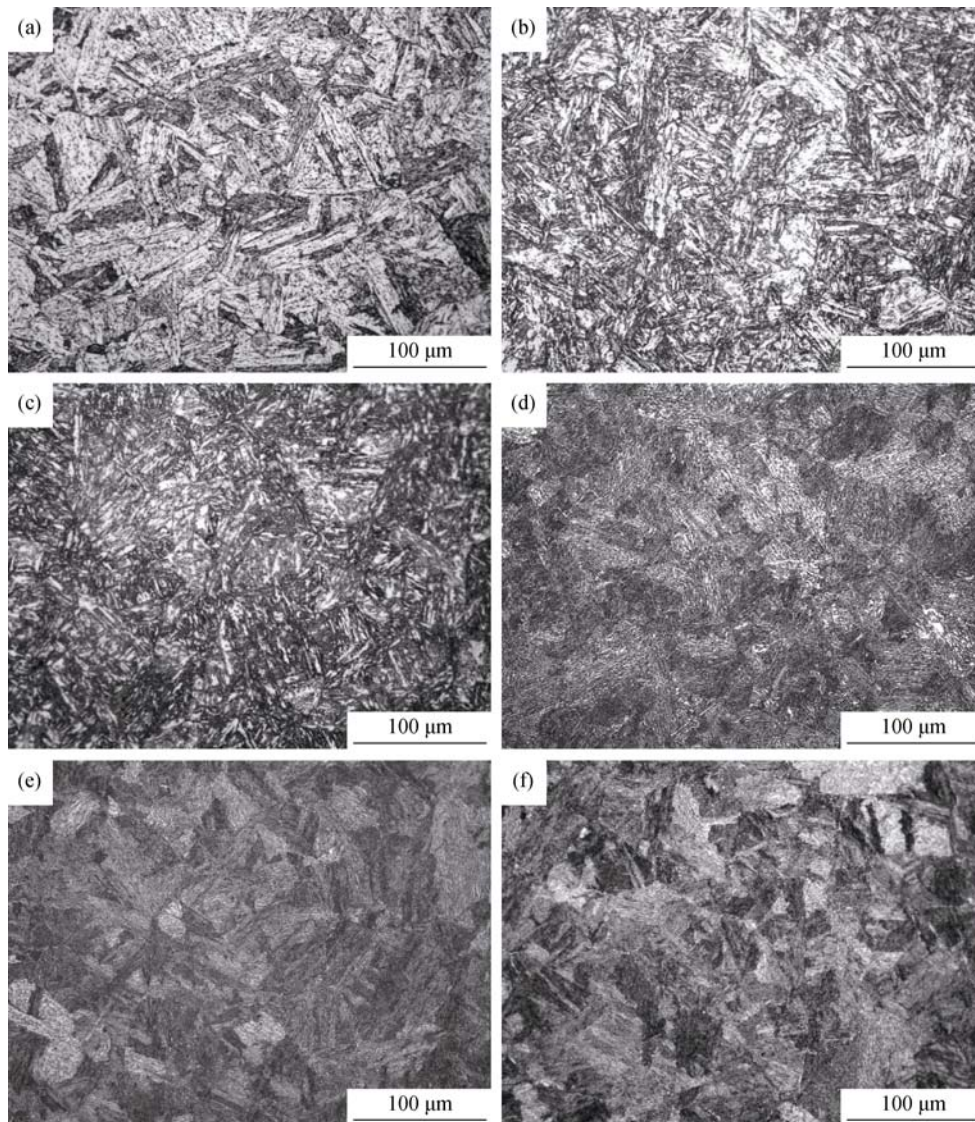


Fig. 4. OM images of the specimens tempered at various temperatures: (a) 570°C; (b) 600°C; (c) 630°C; (d) 650°C; (e) 700°C; (f) 730°C.

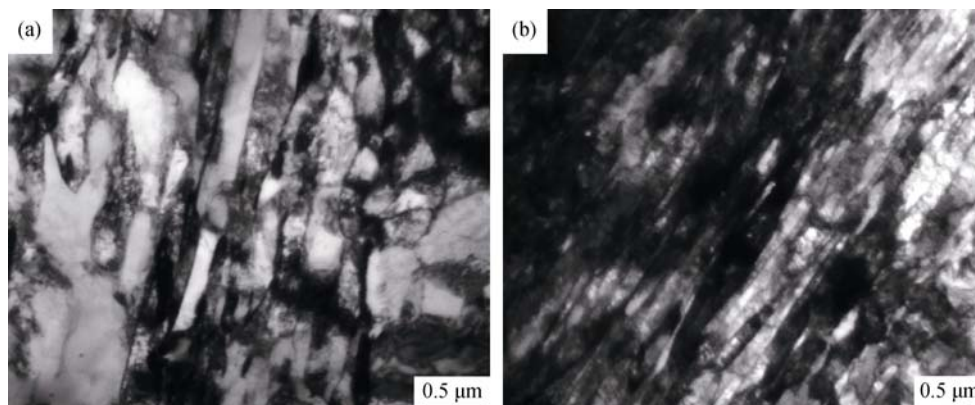


Fig. 5. TEM images of the specimens tempered at (a) 650°C and (b) 730°C for 2 h.

3.3. Tempering at selected temperatures for various periods

To further explore the cause of lath refinement, another

three groups of experiments were conducted, in which specimens were tempered for various periods around the A_s temperature of the steel, at 600°C, 650°C, and 700°C.

(1) Tempering at 600°C.

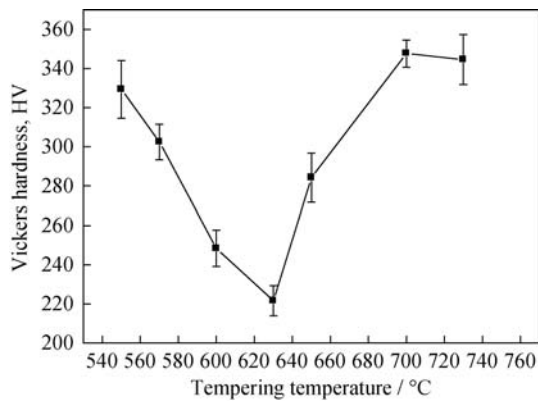


Fig. 6. Variation of Vickers microhardness with tempering temperature for specimens tempered at different temperatures.

In the first group, specimens were tempered at 600°C, which is below A_s temperature, for 2, 4, 6, and 8 h. OM images of the specimens are shown in Fig. 7. As expected, the microstructure remained approximately the same and largely retained the martensite laths. Fig. 8 shows the variation of Vickers microhardness with tempering time for the specimens tempered at 600°C for 2 h, where 0 on the horizontal axis represents the quenched specimen without tempering treatment. The hardness of the specimens decreased steadily as the tempering time prolonged, confirming that no lath refinement occurred during tempering.

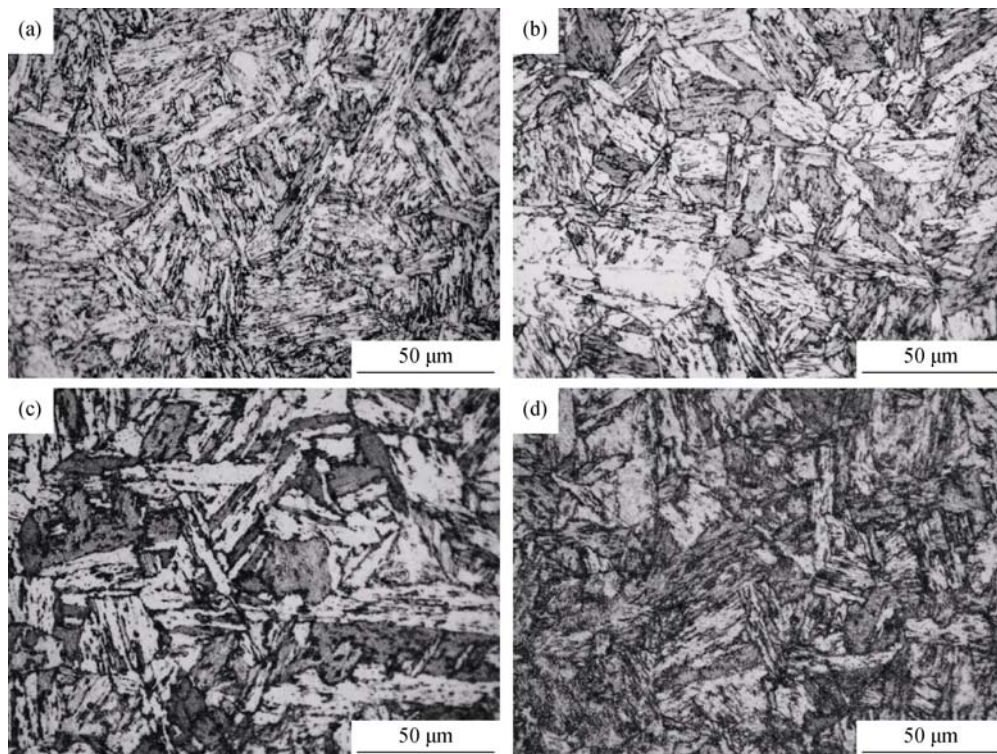


Fig. 7. OM images of the specimens tempered at 600°C for various periods: (a) 2 h; (b) 4 h; (c) 6 h; (d) 8 h.

(2) Tempering at 650°C.

There are two main mechanisms for the α' to γ reverse transformation depending on the heating rate: diffusional and diffusionless [21]. It is demonstrated [21–24] that, below a certain heating rate, the reverse transformation in a number of stainless steels takes place by a thermal-activated diffusional mechanism. In particular, Lee *et al.* [25] found that for a Fe–3Si–13Cr–7Ni (wt%) martensitic stainless steel, the reverse transformation of α' to γ occurs by diffusion when the heating rate is below 600°C/min; otherwise, it occurs by a diffusionless shear mechanism. Considering that all the specimens were heated at a rate of 50–70°C/min, in the current experiment, the reverse transformation of the present steel is of diffusional nature. With the purpose of a better understanding how the diffusional nature of reverse transformation affects the structural refinement and thus, the mechanical properties, a second group of experiments was performed, in which the specimens were tempered at A_s temperature (i.e., 650°C) for 0.5, 1, 2, 4, 6, and 8 h. The OM images of the specimens tempered at 650°C for various periods are shown in Fig. 9. The microstructure of the specimens tempered for 0.5 h and 1 h did not change much, but the martensite laths began to refine and the structure became denser when the steel was tempered for 2 h. As the tempering time increased from 2 h to 8 h, further lath refinement was observed. Similarly, XRD examination was performed on this group of

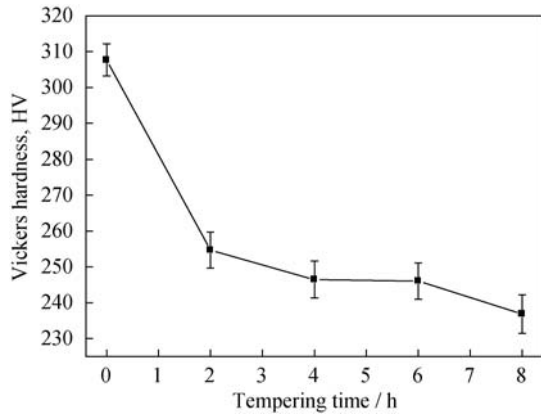


Fig. 8. Variation of Vickers microhardness with tempering temperature for the specimens tempered at 600°C for different periods.

specimens to detect retained austenite in the microstructure. XRD results revealed that retained austenite was present in the specimens tempered for 4 h or longer (Fig. 10). Considering that the volume fraction of the retained austenite was not as large as that of the martensite, the principal peak of the γ phase is barely apparent in the pattern. The retained austenite content calculated according to the previously mentioned equations was plotted against the tempering time (Fig. 11). No austenite phase was detected in the specimens tempered at 650°C for 2 h or shorter. When the tempering time increased to 4 h, the retained austenite became detectable (5.0vol%) and the austenite content increased to 5.3vol% at 6 h and 5.7vol% at 8 h. The variation of the retained austenite content with the tempering time was similar to the results reported by Zou *et al.* [11] and Shirazi *et al.*

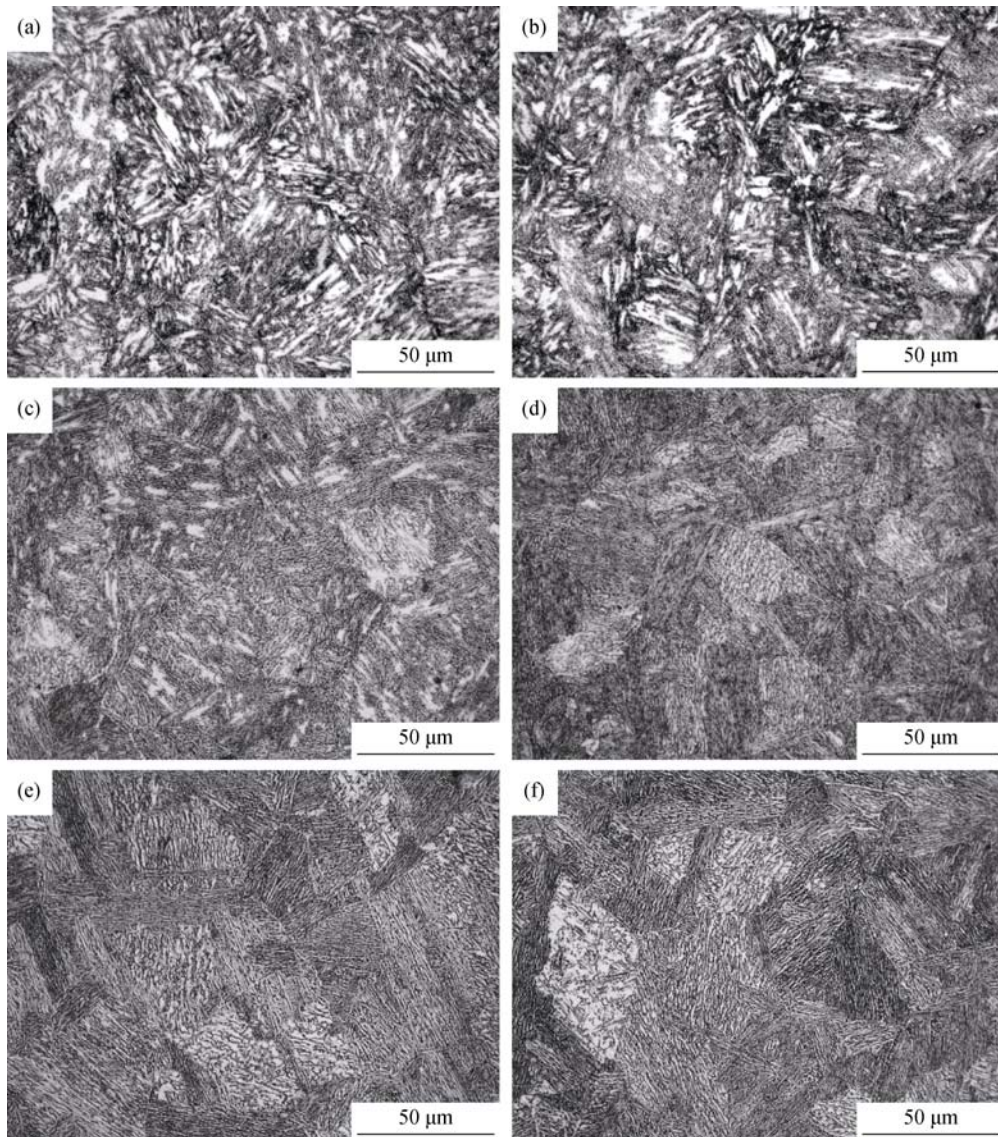


Fig. 9. OM images of the specimens tempered at 650°C for various periods: (a) 0.5 h; (b) 1 h; (c) 2 h; (d) 4 h; (e) 6 h; (f) 8 h.

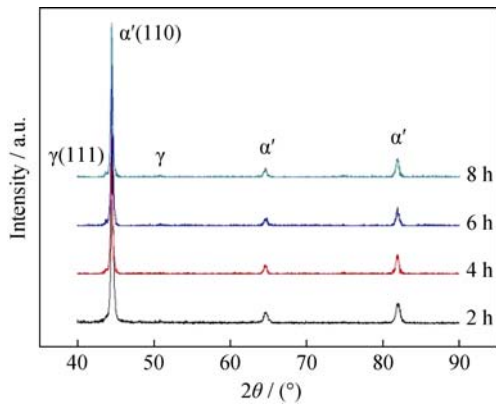


Fig. 10. XRD patterns of the specimens tempered at 650°C for various periods.

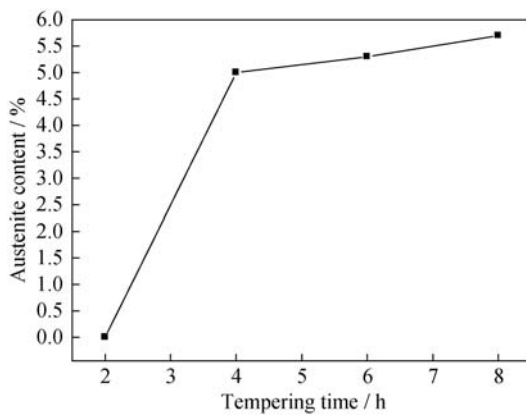


Fig. 11. Variation of austenite content with tempering time for the specimens tempered at 650°C for various periods.

[21], according to which the content of retained austenite at room temperature depends on the stability of reverse austenite [6]. Ni, Si, and Mn enrichment is commonly considered as the major cause of reversed austenite stabilization because these alloying elements significantly decrease the martensite transformation start (M_s) temperature, [26–30].

Fig. 12 shows the variation of Vickers microhardness

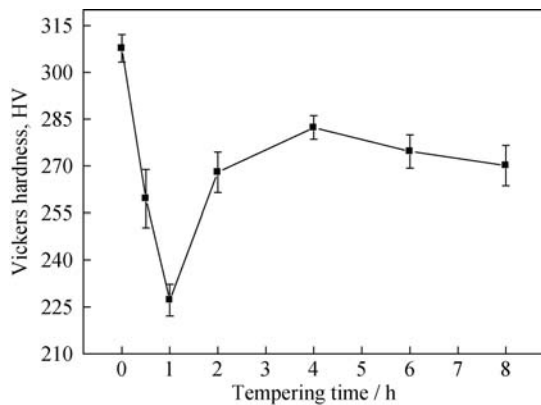


Fig. 12. Variation of Vickers microhardness with tempering temperature for the specimens tempered at 650°C for various periods.

with tempering time for the specimens tempered at 650°C for various periods. The hardness of the specimens tempered for less than 2 h drops in contrast with the previous high value of the quenched specimen, owing to internal stress release and decrease of dislocation density [17–18]. However, there is another increase when the specimen is tempered for 2 h and 4 h, mainly due to martensite refinement. When the tempering time exceeds 4 h, the hardness shows a slight drop, as the content of retained austenite, which is softer than martensite, increases.

(3) Tempering at 700°C.

Because reverse transformation is driven by the diffusional mechanism, the lath refinement can be assumed to proceed faster. Therefore, the tempering temperature was increased to 700°C and the specimens were isothermally held for shorter time than at 650°C to investigate the influence of reverse transformation occurring at a higher temperature on the microstructural evolution. The OM images of the specimens tempered at 700°C for 5, 10, 20, and 30 min are presented in Fig. 13. Packets and blocks of martensite laths within prior austenite grains are still observed with contrast to the specimens tempered for 5 and 10 min. As the tempering time reaches 20 and 30 min, a well-refined microstructure mainly consisting of narrow martensite laths forms. Since reverse transformation takes place following a thermal-activated mechanism, lath refinement is observed in the specimen tempered for only 20 min at 700°C, whereas it occurs at least after 2 h when tempered at 650°C. The variation of Vickers microhardness with tempering time for the specimens tempered at 700°C for various periods is shown in Fig. 14. There is a slight decrease for the specimen tempered for 5 min compared with the quenched specimen; then, different from the specimens tempered at 650°C (Fig. 9), the hardness increases steadily to values higher than that of the original quenched specimen with the tempering time prolonged. The high hardness value was attributed to three reasons. First, Smith *et al.* [31] pointed out that high dislocation density in the reversed austenite, as well as the presence of stacking faults and twins, led to the strength/hardness enhancement of reversed austenite, and thus the newly transformed martensite after cooling. Second, the specimens were tempered for relatively short time at 700°C and, therefore, dislocation recovery and stress release did not take place on a large scale. The resulting hardness decrease, compared to the specimens tempered for long time at 650°C, was thus minimal, although the previous two factors did cause a slight hardness drop for the specimen tempered for 5 min (see Fig. 14). Third, the refined martensite was responsible for about 20 HV hardness increase for the specimen

tempered for 20 min from the original hardness value of 310 HV. As the laths were further refined with the increased

temperature, the hardness of the specimen tempered for 30 min jumped to about 340 HV.

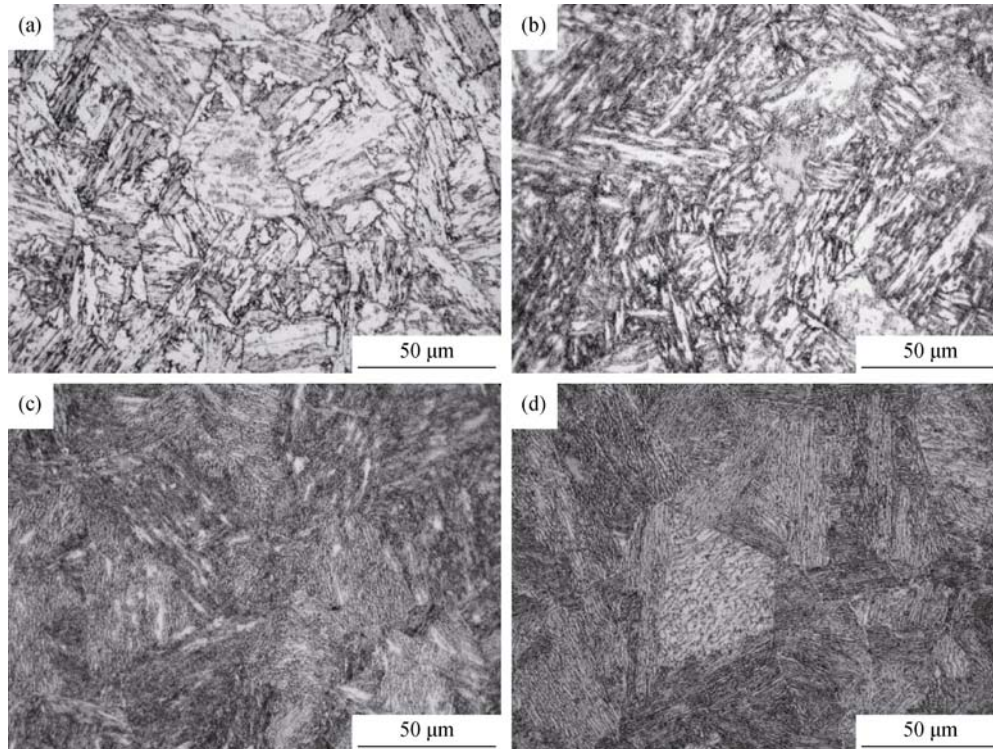


Fig. 13. OM images of the specimens tempered at 700°C for various periods: (a) 5 min; (b) 10 min; (c) 20 min; (d) 30 min.

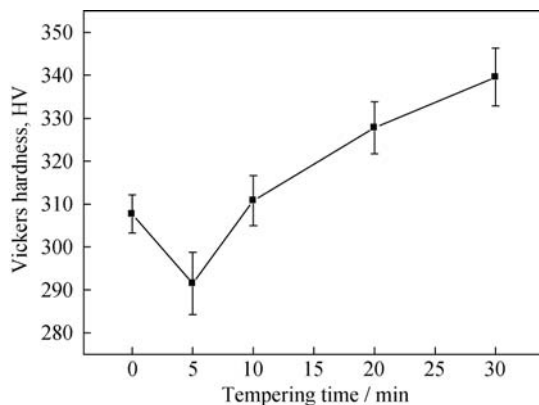


Fig. 14. Variation of Vickers microhardness with tempering time for the specimens tempered at 700°C for various periods.

3.4. Explanation of the structural refinement

Based on other descriptions concerning two-stage tempering of SMSS [8, 14], a schematic diagram was proposed for the martensite lath refinement after intercritical tempering in the present steel. During intercritical tempering, reverse austenite starts to form along the interlath boundaries and grow horizontally at the expense of martensite laths, leading to the reduced width of the original martensite laths;

moreover, the original quenched martensite transforms into tempered martensite. In short time tempering, the α' phase is unlikely to completely transform into the γ phase, and the reversed austenite is thus restrained to narrow stringers between laths [14]. Metastable reversed austenite will re-transform into fresh martensite as the specimen is cooled down to room temperature. Confined by the shape of the reversed austenite, the width of the newly formed martensite laths will be smaller than that of the original ones, thus leading to a structure containing refined martensite. If the tempering time is sufficient for stabilizing elements such as Ni to diffuse and concentrate within part of the reversed austenite, the stabilized part of the reversed austenite will be retained at room temperature in the form of grains between martensite laths after the subsequent cooling [7, 27]. The schematic diagram of the structural refinement due to intercritical tempering is shown in Fig. 15.

4. Conclusions

In the present work, tempering treatment with varying temperature and duration was performed on 00Cr13Ni5Mo2 supermartensitic stainless steel. Specifically, one group of specimens was tempered for 2 h at 570–730°C and another

group was tempered for various periods at 600, 650, and 700°C. Based on the acquired results, the following conclusions were achieved.

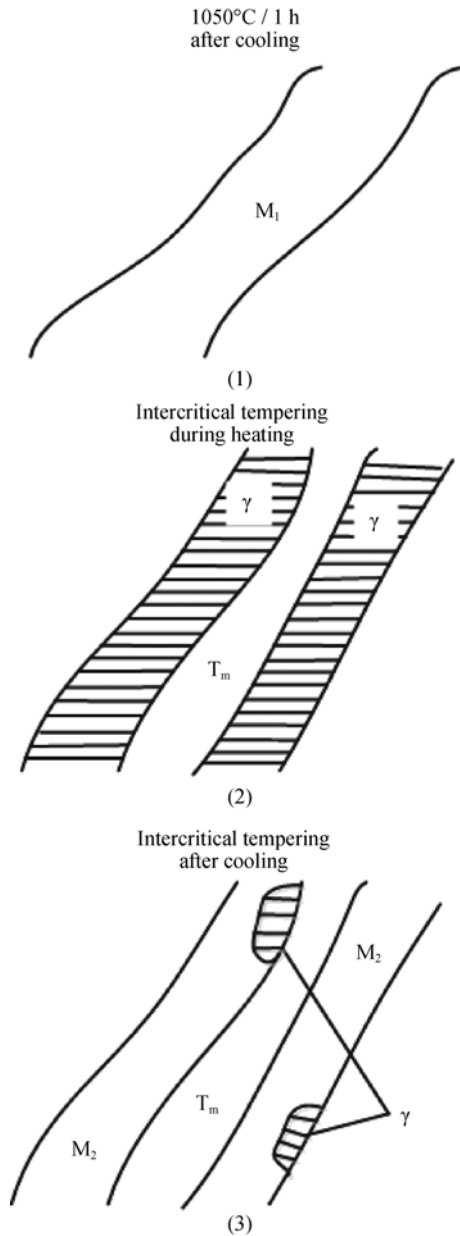


Fig. 15. Scheme of the structural refinement due to single-stage intercritical tempering.

(1) Martensite lath refinement occurs in the specimens tempered above 650°C, which is the austenite transformation start temperature. The lath refinement strongly depends on the tempering time in the intercritical region because it is caused by reverse transformation, which is thought to occur after a diffusional mechanism.

(2) Contrary to the softening effect of normal tempering process, intercritical tempering induced lath refinement and

notably improved the hardness of the steel. This enhancement effect is stronger for tempering at 700°C than for tempering at 650°C.

(3) Retained austenite content exhibits a steady increase with increasing tempering time at 650°C, while no retained austenite is detected in the specimens tempered at 700°C.

Acknowledgements

The authors are grateful to the Major State Basic Research Development Program of China (No. 2014CB046805) and China National Funds for Distinguished Young Scientists (No. 51325401) for grant and financial support.

References

- [1] A. Bojack, L. Zhao, P.F. Morris, and J. Sietsma, *In-situ* determination of austenite and martensite formation in 13Cr6Ni2Mo supermartensitic stainless steel, *Mater. Charact.*, 71(2012), p. 77.
- [2] P.D. Bilmes, C.L. Llorente, C.M. Méndez, and C.A. Gervasi, Microstructure, heat treatment and pitting corrosion of 13CrNiMo plate and weld metals, *Corros. Sci.*, 51(2009), No. 4, p. 876.
- [3] B. Qin, Z.Y. Wang, and Q.S. Sun, Effect of tempering temperature on properties of 00Cr16Ni5Mo stainless steel, *Mater. Charact.*, 59(2008), No. 8, p. 1096.
- [4] Y.Y. Song, D.H. Ping, F.X. Yin, X.Y. Li, and Y.Y. Li, Microstructural evolution and low temperature impact toughness of a Fe–13%Cr–4%Ni–Mo martensitic stainless steel, *Mater. Sci. Eng. A*, 527(2010), No. 3, p. 614.
- [5] Y.Y. Song, X.Y. Li, L.J. Rong, and Y.Y. Li, Anomalous Phase Transformation from martensite to austenite in Fe–13%Cr–4%Ni–Mo martensitic stainless steel, *J. Mater. Sci. Technol.*, 26(2010), No. 9, p. 823.
- [6] M. De Sanctis, R. Valentini, G. Lovicu, A. Dimatteo, R. Ishak, U. Migliaccio, R. Montanari, and E. Pietrangeli, Microstructural evolution during tempering of 16Cr–5Ni stainless steel: effects on final mechanical properties, *Mater. Sci. Forum*, 762(2013), p. 176.
- [7] Y.Y. Song, X.Y. Li, L.J. Rong, and Y.Y. Li, The influence of tempering temperature on the reversed austenite formation and tensile properties in Fe–13%Cr–4%Ni–Mo low carbon martensite stainless steels, *Mater. Sci. Eng. A*, 528(2011), No. 12, p. 4075.
- [8] P.D. Bilmes, M. Solari, and C.L. Llorente, Characteristics and effects of austenite resulting from tempering of 13Cr–NiMo martensitic steel weld metals, *Mater. Charact.*, 46(2001), No. 4, p. 285.
- [9] X.P. Ma, L.J. Wang, C.M. Liu, and S.V. Subramanian, Role of Nb in low interstitial 13Cr super martensitic stainless steel, *Mater. Sci. Eng. A*, 528(2011), No. 22–23, p. 6812.
- [10] X.P. Ma, L.J. Wang, C.M. Liu, and S.V. Subramanian, Micro-

- structure and properties of 13Cr5Ni1Mo0.025Nb0.09V0.06N super martensitic stainless steel, *Mater. Sci. Eng. A*, 539(2012), p. 271.
- [11] D.N. Zou, Y. Han, W. Zhang, and X.D. Fang, Influence of tempering process on mechanical properties of 00Cr13Ni4Mo supermartensitic stainless steel, *J. Iron Steel Res. Int.*, 17(2010), No. 8, p. 50.
- [12] C.A.D. Rodrigues, P.L.D. Lorenzo, A. Sokolowski, C.A. Barbosa, and J.M.D.A. Rollo, Titanium and molybdenum content in supermartensitic stainless steel, *Mater. Sci. Eng. A*, 460–461(2007), p. 149.
- [13] Y.R. Liu, D. Ye, Q.L. Yong, J. Su, K.Y. Zhao, and W. Jiang, Effect of heat treatment on microstructure and property of Cr13 super martensitic stainless steel, *J. Iron Steel Res. Int.*, 18(2011), No. 11, p. 60.
- [14] J. Hubáčková, V. Číhal, and K. Mazanec, Two-stage tempering of steel 13%Cr6%Ni, *Materialwiss. Werkstofftech.*, 15(1984), No. 12, p. 411.
- [15] M. Tanaka and C. Choi, Effects of C contents and Ms temperatures on the hardness of martensitic Fe–Ni–C alloys, *Trans. Iron Steel Inst. Jpn.*, 12(1972), No. 1, p. 16.
- [16] E.S. Park, D.K. Yoo, J.H. Sung, C.Y. Kang, J.H. Lee, and J.H. Sung, Formation of reversed austenite during tempering of 14Cr–7Ni–0.3Nb–0.7Mo–0.03C super martensitic stainless steel, *Met. Mater. Int.*, 10(2004), No. 6, p. 521.
- [17] M. Al Dawood, I.S. El Mahallawi, M.E. Abd El Azim, and M.R. El Koussy, Thermal aging of 16Cr–5Ni–1Mo stainless steel: Part 1. Microstructural analysis, *Mater. Sci. Technol.*, 20(2004), No. 3, p. 363.
- [18] M. Al Dawood, I.S. El Mahallawi, M.E. Abd El Azim, and M.R. El Koussy, Thermal aging of 16Cr–5Ni–1Mo stainless steel: Part 2. Mechanical property characterisation, *Mater. Sci. Technol.*, 20(2004), No. 3, p. 370.
- [19] T.H. Lee, S.J. Kim, and Y.C. Jung, Crystallographic details of precipitates in Fe–22Cr–21Ni–6Mo–(N) superaustenitic stainless steels aged at 900°C, *Metall. Mater. Trans. A*, 31(2000), No. 7, p. 1713.
- [20] W.J. Hui, *Ultra-Fine Grained Steels*, Springer, Berlin, Heidelberg, 2009, p. 300.
- [21] H. Shirazi, G. Miyamoto, S. Hossein Nedjad, H. Ghasemi-Nanesa, M. Nili Ahmadabadi, and T. Furuhaara, Microstructural evaluation of austenite reversion during intercritical annealing of Fe–Ni–Mn martensitic steel, *J. Alloys Compd.*, 577(2013), No. Suppl. 1, p. 572.
- [22] C.A. Apple and G. Krauss, The effect of heating rate on the martensite to austenite transformation in Fe–Ni–C alloys, *Acta Metall.*, 20(1972), No. 7, p. 849.
- [23] D.S. Leem, Y.D. Lee, J.H. Jun, and C.S. Choi, Amount of retained austenite at room temperature after reverse transformation of martensite to austenite in an Fe–13%Cr–7%Ni–3%Si martensitic stainless steel, *Scripta Mater.*, 45(2001), No. 7, p. 767.
- [24] R. Kapoor, L. Kumar, and I.S. Batra, A dilatometric study of the continuous heating transformations in 18wt% Ni maraging steel of grade 350, *Mater. Sci. Eng. A*, 352(2003), No. 1–2, p. 318.
- [25] Y.K. Lee, H.C. Shin, D.S. Leem, J.Y. Choi, W. Jin, and C.S. Choi, Reverse transformation mechanism of martensite to austenite and amount of retained austenite after reverse transformation in Fe–3Si–13Cr–7Ni (wt%) martensitic stainless steel, *Mater. Sci. Eng. A*, 19(2003), No. 3, p. 393.
- [26] L. Liu, Z.G. Yang, and C. Zhang, Effect of retained austenite on austenite memory of a 13% Cr–5% Ni martensitic steel, *J. Alloys Compd.*, 577(2013), No. Suppl. 1, p. 654.
- [27] Y.Y. Song, X.Y. Li, L.J. Rong, D.H. Ping, F.X. Yin, and Y.Y. Li, Formation of the reversed austenite during intercritical tempering in a Fe–13%Cr–4%Ni–Mo martensitic stainless steel, *Mater. Lett.*, 64(2010), No. 13, p. 1411.
- [28] H. Chen, M. Gouné, and S. van der Zwaag, Analysis of the stagnant stage in diffusional phase transformations starting from austenite-ferrite mixtures, *Comput. Mater. Sci.*, 55(2012), p. 34.
- [29] H. Chen, R. Kuziak, and S. van der Zwaag, Experimental evidence of the effect of alloying additions on the stagnant stage length during cyclic partial phase transformations, *Metall. Mater. Trans. A*, 44(2013), No. 13, p. 5617.
- [30] L.J. Wang, Q.W. Cai, H.B. Wu, and W. Yu, Effects of Si on the stability of retained austenite and temper embrittlement of ultrahigh strength steels, *Int. J. Miner. Metall. Mater.*, 18(2011), No. 5, p. 543.
- [31] H. Smith and D.R.F. West, The reversion of martensite to austenite in certain stainless steels, *J. Mater. Sci.*, 8(1973), No. 10, p. 1413.